

Thermo-kinetics study of orange peel in air

B. Zapata · J. Balmaseda · E. Fregoso-Israel ·
E. Torres-García

Received: 20 January 2009 / Accepted: 3 April 2009 / Published online: 12 August 2009
© Akadémiai Kiadó, Budapest, Hungary 2009

Abstract Thermal degradation of orange peel was studied in dynamic air atmosphere by means of simultaneous TG-DSC and TG-FTIR analysis. According to the obtained thermal profiles, the orange peel degradation occurred in at least three steps associated with its three main components (hemicellulose, cellulose and lignin). The volatiles compounds evolved out at 150–400 °C and the gas products were mainly CO₂, CO, and CH₄. A mixture of acids, aldehydes or ketones C=O, alkanes C–C, ethers C–O–C and H₂O was also detected. The E_a on α dependence revealed the existence of different and simultaneous processes suggesting that the combustion reaction is controlled by oxygen accessibility, motivated by the high evolution low-molecular-mass gases and volatile organic compounds. These results could explain the non-autocatalytic character of the reactions during the decomposition process.

Keywords Combustion kinetics · Biomass · Orange peel · TG-FTIR · Thermal analysis

Introduction

The use of biomass as an energy source is of great importance, because it can be converted into useful energetic products or into valuable chemicals [1–3]. Thus, the

study of its properties from the point of view of combustion, pyrolysis, gasification, and other thermochemical utilization processes is an important research direction [4]. Although, the biomass conversion has been actively studied, there is a wide variety of biomass-type that has not been yet tested. In general, biomass contains different components, such as starch, cellulose, hemicellulose, and lignin, together with trace amounts of extractives and minerals [5, 6]. In terms of thermal stability, it has been established the following order of degradation of the main components of biomass: hemicellulose > cellulose > lignin [7]. Several studies on these components have been reported, because to the possibility of convert them into a wide range of liquid fuels, called frequently “biofuels”, such as bioethanol or biodiesel [8].

Even though the biomass combustion process is not recommended, it is widely used for energy production of agricultural wastes [5, 9]. Particularly, the information about biomass combustion kinetics is necessary to accurately predict reactions behavior as well as to optimize the process of combustion of the different products during the decomposition. Thus, the thermogravimetric analysis (TG) is one of the most commonly used techniques to study the different parameters on combustion behavior and reaction kinetics [10–12].

In the present work, the thermal decomposition of orange peel under ultra dry air atmosphere has been examined and a detailed analysis of the gases released during thermal study was carried out. Several measurements have been run on orange peel at different heating rate from room temperature to 700 °C. Then a model-free kinetics approach has been applied to data for non-isothermal degradation of orange peel.

Regardless of the extensive studies on thermal degradation of different biomass sources, a scarce attention has

B. Zapata · E. Torres-García (✉)
Instituto Mexicano del Petróleo, Eje Central # 152,
07730 Mexico, DF, Mexico
e-mail: etorresg@imp.mx

J. Balmaseda · E. Fregoso-Israel
Departamento de Polímeros, Instituto de Investigaciones en
Materiales, Universidad Nacional Autónoma de México,
C.P. 04510 Mexico DF, Mexico

been focused to orange peel. To our knowledge, this is the first thermo-kinetics systematical study of thermal degradation of orange peel.

Experimental

Orange peel sample was exposed under several treatments before analysis. Firstly, it was dried at room temperature during 15 days. Secondly, it was dried in a furnace at 120 °C in air flow for 24 h. Finally, the orange peel was ground in a laboratory-scale ball mill and sieved to obtain about 0.1–0.3 mm size. The moisture content after these three steps was 2.7%, determined at 100 °C via TG.

The elemental analysis was performed in a CHN/O Vario EL analyzer using the ASTM D5291 method. The sulfur content was determined in HORIBA SLFA-1800 equipment with ASTM D4294 method. Ash content was obtained by using the ASTM D482 method by Limberth muffle use. Chlorine content was measured in a Mitsubishi X-10 by using the EPA 953 method. The oxygen content was obtained by a mass balance between C, H and N. The chemical structure of the original orange peel waste sample was identified using infrared spectroscopy. The sample was mixed with KBr powder and was dried in the oven at 100 °C for 24 h.

Thermal degradation of orange peel was first carried out in a simultaneous TGA-DSC (NEZTZSCH STA 409 PC). To mitigate the difference of heat and mass transfer, the sample mass was kept at ~12 mg. The samples were heated from room temperature up to 700 °C at a constant heating rate of 10 °C min⁻¹, using an ultra dry air atmosphere and a flow rate of 100 mL min⁻¹.

Analysis of the gases released during thermal decomposition was carried out in a TGA (TA Instrument's 2950). The gases released in the TG experiments were swept immediately to a gas cell, followed by the FT-IR (NICOLET Protégé 460 spectrometer) analysis. The transfer line and gas cell were heated to an internal temperature of 240 °C, to avoid condensation or adsorption of semi-volatile products. Each IR spectrum was recorded at 5 s and the IR scanning range was from 4000 to 500 cm⁻¹.

TG measurements were performed at different heating rates of 2, 5 and 10 °C min⁻¹ and the DTG data collected at different heating rates were used to obtain information on the amount and nature of the different process and to estimate the activation energy involved in each stage and its dependence on the degree of reaction extent α . The mass samples were about 12 mg in all cases and the sensitivity of the balance was 10⁻⁷ g.

Results and discussion

Chemical composition of orange peel

The properties of the orange peel used in this study are shown in Table 1.

Chemical structure of orange peel

Figure 1 shows the FTIR spectrum of the dried orange peel waste. The spectrum presents the characteristic bands corresponding to cellulose besides of lignin [13]. The most intense band in the high energy region is due to a large amount of OH groups of the carbohydrates and those of lignin. The intense band at 1045 cm⁻¹ corresponds to the link C–O–H or C–O–R (alcohols or esters) while the distinctive band at 2925 cm⁻¹ is related to the presence of C–H stretching vibration together with bending vibrations around 1428 cm⁻¹ of aliphatic chains (–CH₂– and –CH₃–) forming the basic structure of this lignocellulosic materials [14]. The signal at 1736 cm⁻¹ can be assigned to carbonyl

Table 1 Elemental analyses and water content of the orange peel

Chemical components	Mass/%
Carbon	49.59
Hydrogen	6.95
Oxygen	39.7
Nitrogen	0.66
Sulfur	0.06
Chloride	0.001
Ash	3.05
Water	2.73

The oxygen content is calculated by difference

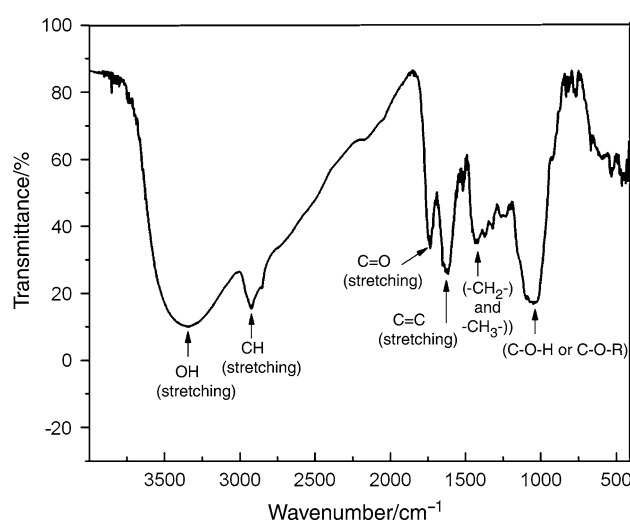


Fig. 1 FTIR spectrum of the dried orange peel sample

groups presence like ester. Finally, the band at around 1617 cm^{-1} can be attributed to aliphatic and/or unsaturated aromatic compounds [15].

Thermal study

The typical thermal profile of the orange peel, obtained by simultaneous TG-DSC in ultra dry air, is shown in Fig. 2. In general, at least five main thermal events can be clearly distinguished up to $600\text{ }^\circ\text{C}$. It can be observed that the sample mass decreases continuously between room temperature and $580\text{ }^\circ\text{C}$, which is related to dehydration process and thermal degradation of the orange peel. The initial mass loss ($2.73\text{ mass}\%$), below of $100\text{ }^\circ\text{C}$, is associated with the release of weakly bonded water molecule (physical adsorbed water molecules). While the main mass losses at 212 , 310 , 443 – 466 and $527\text{ }^\circ\text{C}$ (see DTG curve) are associated to the biomass decomposition, essentially, to its three main components (hemicellulose, cellulose and lignin) [6, 16]. Correspondingly, DSC curve shows at least five events maximized about ~ 215 , ~ 302 , ~ 432 , ~ 468 and $515\text{ }^\circ\text{C}$. All these thermal events are exothermal character, except the related water release at $85\text{ }^\circ\text{C}$.

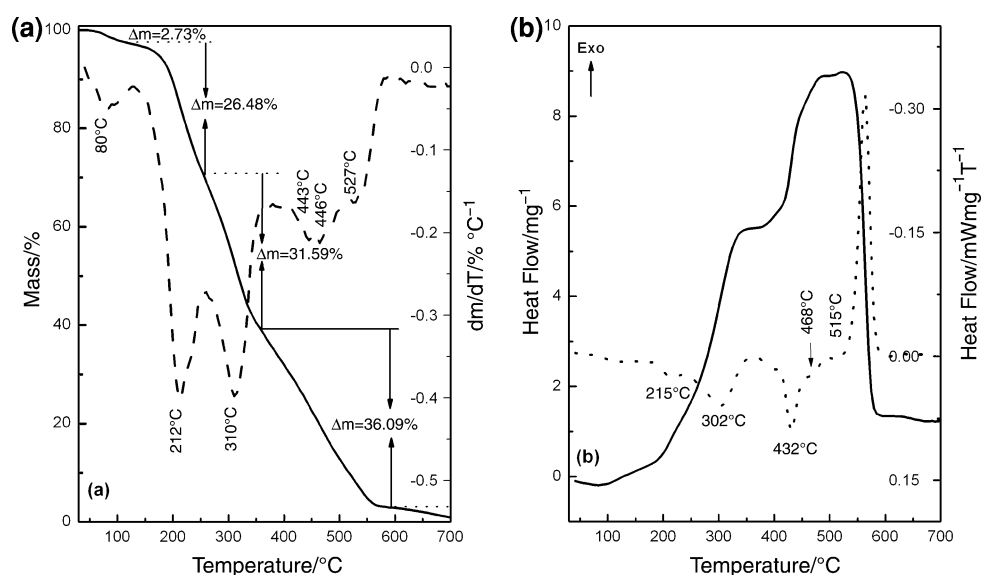
Once the physically bonded water evolved, at least five thermal processes are detected in the TG-DTG and DSC/DDSC curves (Fig. 2a, b). The thermal profile of these stages reveals the presence of several simultaneous and complex processes. The dehydrated biomass is stable up to $140\text{ }^\circ\text{C}$, and then begins to decompose. The first step, from 150 to $255\text{ }^\circ\text{C}$, characterized by an exothermic peak at $215\text{ }^\circ\text{C}$ agrees with the mass loss of $26.5\text{ mass}\%$ and is attributed to the degradation of hemicelluloses. Hemicellulose is a mixture of various polymerized monosaccharides, such as glucose, mannose, galactose, xylase, arabinose

among others, with lower molecular mass and lower thermal stability than cellulose. Hemicelluloses decompose at temperature of 200 – $260\text{ }^\circ\text{C}$, giving rise to more volatiles, less tars, and less chars than cellulose [6]. The contiguous and/or simultaneous processes between 260 and $360\text{ }^\circ\text{C}$ show an exothermic peak at $302\text{ }^\circ\text{C}$, associated to a mass loss of $31.6\text{ mass}\%$ due to the degradation of cellulose. Cellulose forms long chains that are bonded to each others by a long network of hydrogen bonds. Groups of cellulose chains twist in space to make up ribbonlike microfibril sheets, which are the basic construction units for a variety of complex fibers. As a consequence, their crystalline structure resists thermal decomposition better than hemicelluloses [6, 13].

Finally, three overlap processes in the temperature interval from 380 to $585\text{ }^\circ\text{C}$ can be distinguished, which are identified on DTG curve at ~ 443 , ~ 466 and $527\text{ }^\circ\text{C}$. The total mass loss up to $585\text{ }^\circ\text{C}$ relative to the initial mass for these last three stage was of $36.1\text{ mass}\%$. It might be attributed essentially to a degradation step of lignin and char or tar residues, where the homologous phenolic compounds could be the main product [6, 17]. Lignin is an amorphous cross-linked resin with no exact structure and its degradation occurs between 280 and $500\text{ }^\circ\text{C}$. In addition, lignin is the main responsible for char production. In this case, the analysis is especially difficult due to the formation of complex phenolic species during lignin decomposition.

It is interesting to note that the degradation studies on separated lignin will not necessarily match the thermal behavior of this component when it is present in the original biomass. In general, the exothermic character of the DSC events accompanying the biomass decomposition step is related to the oxidation of different organic compounds to CO_2 , CO , and H_2O , which is the common fact in thermal decomposition of biomass in air atmosphere.

Fig. 2 TG-DTG and DSC-DDSC curves of orange peel in air atmosphere at heating rate of $10\text{ }^\circ\text{C min}^{-1}$



Evolved gas analysis during thermal decomposition

During the thermal decomposition the gases released in the TG were swept immediately to a gas cell, followed by FTIR analysis (see changes in IR intensity as a function of temperature, Fig. 3a). The IR spectra during the most important thermal events are shown in the Fig. 3b. The typical functional groups are indicated on IR spectrum in the different thermal intervals. The releasing of the gas products mainly focused at low temperature (150–600 °C), corresponding this temperature range to a high formation of gas product according to our results.

The changes in IR peak intensity reflect the tendency of concentration variation of the gaseous species, as a function of temperature. The specific wave numbers of the IR peaks of the main gaseous species from orange peel highlight CO and CO₂ formation in all cases for temperature ($T > 150$ °C), which indicates that, in presence of air (21% O₂), complete or partial oxidation is an eventual reaction pathway. Therefore, peaks appearing at 2365 and 3327 cm⁻¹ correspond to CO₂ and those at 2186 and 2100 cm⁻¹ are attributed to CO. It is interesting to note that at temperature higher than 550 °C, the release of CO₂ and CO decreased with temperature, suggesting the end of the decomposition reaction.

Peaks between ~ 3760 and 3580 cm⁻¹ are assigned to the symmetric and asymmetric stretch vibrations that are associated with H₂O molecules. While the signals about 3700–3900 cm⁻¹, may correspond to a rota-vibrational band of water vapor [18]. Furthermore, the peak around 1640 cm⁻¹ was assigned to the bending mode vibration of H₂O molecules.

On the other hand, the C–H stretching vibrations between 1350 and 1475 cm⁻¹ indicated the presence of alkanes. Meanwhile, the peaks in the range of ~ 3000 – 2700 cm⁻¹ are assigned essentially to CH₄ stretch

vibration. It is well-known that the peaks in the FTIR spectrum at ~ 3000 – 2700 cm⁻¹ also can be assigned to a products mixture consistent of C₃H₈, C₂H₆, C₂H₄ and C₂H₂ and that the change in absorption intensity may be due to the relative change in concentration of the produced CH groups in presence of O₂ [19].

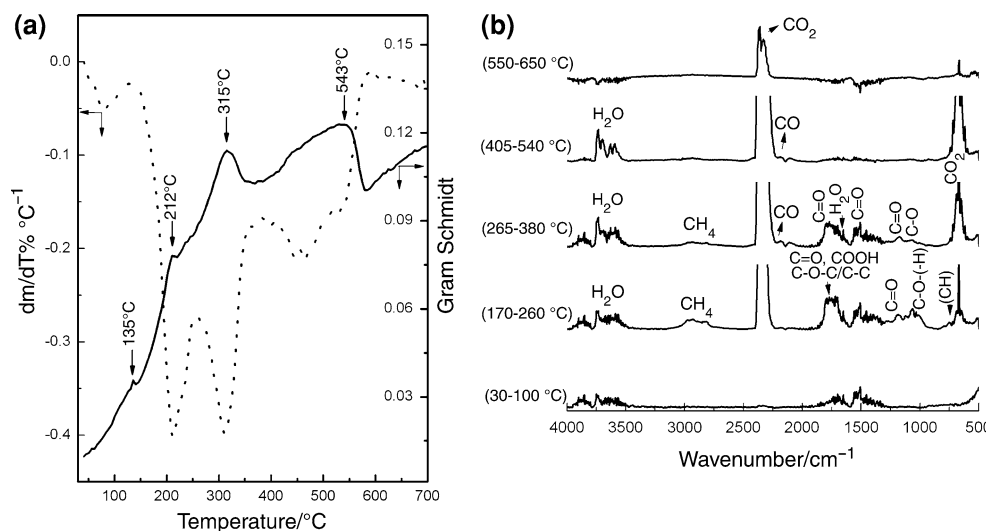
The evolution of H₂O, CH₄ and volatiles (organic products mixture) was increased and reach its maximum between 150 and 400 °C. The presence of different oxygen-containing functional groups, besides H₂O, CO and CO₂, are observed between 1765–1715 and 1505–1560 cm⁻¹, as well as, at 1176 and 1030 cm⁻¹. The band located at 1030 cm⁻¹ can be attributed to alcohols C–O–(H) formed during the conversion process. Meanwhile, absorption at 1176 cm⁻¹ can be assigned to C=O stretching vibration, and in the present case, it is most likely from carboxylic acids. Note that the C=O stretch vibrations corresponding to aldehydes are typically observed in the range of 1735 cm⁻¹ [19]. Finally, with regards to the peaks about 1765–1715 and 1560–1505 cm⁻¹, those can be associated with the cracking of carbohydrate contained organic functional groups (C=O; C–O–C/C–C; and COOH) [13].

Up to this point, we can conclude that the gas products during the orange peel degradation are mainly CO₂, CO, CH₄ and some organics, a mixture of acids, aldehydes or ketones (C=O), alkanes (C–C) and ethers (C–O–C) with some H₂O.

Kinetics analysis

A series of DTG curves in dynamic air atmosphere of the thermal decomposition of orange peel at different heating rate appear in Fig. 4. Thermal profiles of the biomass decomposition can be interpreted as a multiple and simultaneous processes, which difficult their assignation and understanding. For better clarity, the TG curves are

Fig. 3 **a** Changes in IR intensity (Gram Schmidt) and its relationships with dm/dT as a function of temperature. **b** Typical FTIR spectra of gaseous species produced from orange peel during its degradation under ultra dry air to different intervals temperature



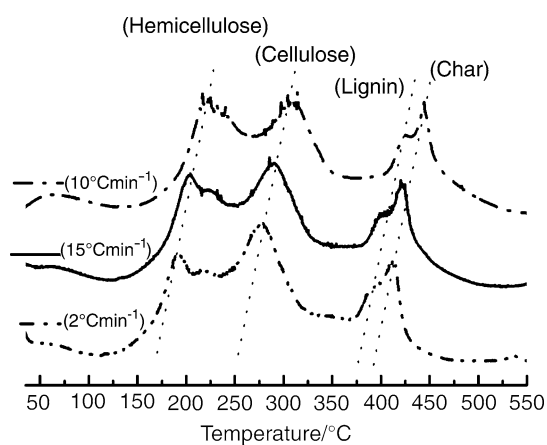


Fig. 4 Effect of heating rate on the DTG curves

represented in their derivative form DTG. In all cases it was observed that an increase in the heating rate shifts the DTG curves and peak temperature to higher values. This indicated that the reaction rate is only function of the temperature, at least under the experimental conditions used in this study.

Model-free isoconversion method

The DTG data collected at different heating rates were processed according to the isoconversion method in order to obtain the dependence of the activation energy E_x as a function of transformation degree α [20–22]. This method is based on the isoconversional principle that states that the reaction rate at constant extent of conversion is only a function of temperature

$$\left[\frac{d \ln \left(\frac{dx}{dt} \right)}{dT^{-1}} \right]_{\alpha} = - \frac{E_x}{R} \quad (1)$$

where the subscript α denote at a specific extent of reaction, t is time, T is absolute temperature, R is the gas constant and E_x is the activation energy as a function of the extent of degradation. This criterion allows an estimation of energy E_x without the assumption of any reaction model.

For this purpose, the different thermal events (Fig. 4) were separate by stages (starting of its DTG curves) to visualize its different nature according to the measured dynamic property (mass) and the energetic dependence of E_x with α for each process is shown in Fig. 5. From these results, it was possible to analyze the degradation process of the biomass (orange peel) and establish some considerations on the experimental conditions and most probable mechanisms.

Analysis in terms of activation energy shows the complex E_x on α dependence and reveal the energetic behavior of the different thermal events during the degradation of orange peel in air atmosphere.

The analyses of the E_x versus α associated to hemicellulose degradation (between 90 and 100 kJ mol⁻¹),

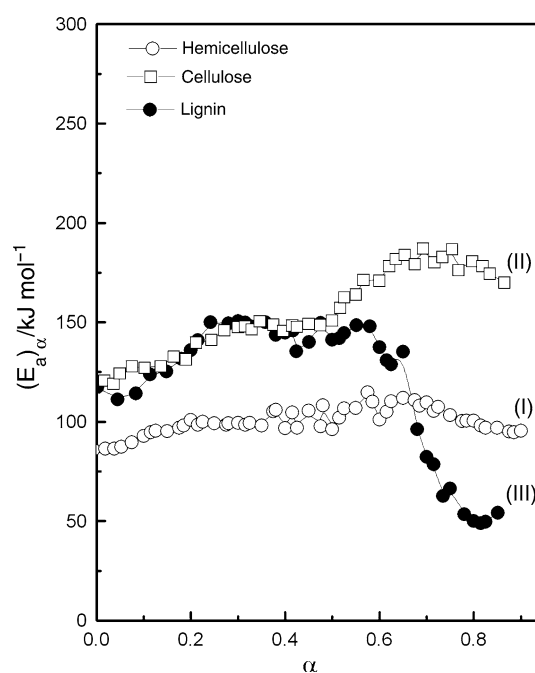


Fig. 5 Effective activation energy as a function of the extent of reaction, determined by the isoconversion method during thermal decomposition of the orange peel

curve (I), shows that the activation energy is essentially independent of extent of reaction α . This result suggests that the chemical nature of the processes during this stage are not significantly different, and that changes of the E_x as a function of the extent of degradation α does not represent important modifications in the reaction mechanism; i.e., the step that always limits the speed of the reaction is in general the same, which, however, does not exclude other simultaneous mechanisms. Therefore, we can only suggest that the involve process are very similar energetically, at least under our experimental conditions used.

Results on the E_x versus α dependence for the cellulose degradation curve (II), show that the activation energy presents variations between 120 and 190 kJ mol⁻¹ for all transformation ranges. At least three thermal processes, with slope changes of about $\alpha \approx 0.25$, and 0.5 are detected, illustrating the complex contributions of all the chemical constituents. Therefore, the presences of these zones are a clear indication of the different chemical processes and can be associated to a change in the reaction mechanism. The fact that the activation energy, during this process increases as the decomposition advances (see Fig. 5, curve II) might be attributed to the cracking of some functional groups, structural depolymerization and chains breaking in cellulose residue [6, 13]. When the chains break they become shorter and as a consequence more stables, then a higher activation energy would be needed to initiate any process. This result reveals typical behavior for competitive reaction [23].

On the other hand, during the last stage, associated to lignin degradation process (curve III), were also detected different changes undergone by the E_x . The activation energy was changing from 115 to 140 kJ mol⁻¹ in the range of α values of 0–0.6. Afterwards, in the range, $0.62 \leq \alpha \leq 0.90$, the activation energy decreased, from 140 up to 51 kJ mol⁻¹ near the end of the reaction. This last stage probably might be attributed to the secondary decomposition (thermal cracking of tar residue and/or char combustion), while, the decreasing in activation energy would be associated to the easy oxygen accessibility on the residual solid, which promotes the combustion of the residual solid. This is consistent with the lower concentration of gas products evolving from biomass degradation at temperatures higher than 400 °C.

The results suggest that, under experimental conditions used in this study, the mass transfer phenomena are essential during combustion process and, in all cases the dependence of E_x as a function of the extent of degradation α is probably a typical reaction controlled by the accessibility of the oxygen toward the direct vicinity of the residual solid, except the related thermal cracking of tar residue and/or char combustion.

This approach suggest that at least during the previous stages of degradation the high evolution gaseous products, such as, H₂O, CH₄, CO₂, CO and volatile organic compounds, apparently controls the reaction rate, limiting the oxygen accessibility towards the residual solid and promoting the reaction preferentially in gas phase. It explains why the reactions are not thermally auto-catalyzed.

A more detailed study for each stage is difficult due to several simultaneous and complex processes occurring. These processes can include cracking of functional groups, depolymerization, volatilization reactions, bond rupture, adsorption and diffusion, among others. Obviously, the modification of any experimental parameter can generate pressure and temperature gradients which modify the thermal profile and the kinetic parameters, affecting the conversion of biomass into useful forms of energy. All these considerations make any kinetic study difficult because the possible kinetic evaluation for a biomass (in this particular case, orange peel) will have only a global or apparent character without a clear physical or chemical meaning.

Conclusions

Thermal degradation of orange peel was studied in dynamic air atmosphere and their thermo-kinetic parameters and gas product distribution were analyzed.

The present study using TG-FTIR and thermo-kinetic characterization during thermal degradation of orange peel,

suggest that degradation process occurs in at least three main steps, between 150 and 600 °C and the gas evolved comprised mainly CO, CO₂, CH₄, light hydrocarbons with some H₂O.

- In the temperature range of 150–250 °C, hemicellulose degradation takes place, probably by depolymerization and thermal cracking of functional groups, such as carbonyl groups.
- Subsequently, between 250 and 360 °C, depolymerization, defunctionalization and chains breaking of cellulose occur, evolving low-molecular-mass gases, such as CO₂, CO, CH₄, H₂O and volatiles (organic compounds mixture).
- Finally, three overlapped processes from 380 to 585 °C are assigned to lignin degradation with formation of complex phenolic species, thermal cracking of tar residue and combustion of char.

The isoconversional analysis shows the complex E_x on α dependence and reveals the existence of different and simultaneous processes. In general, this study suggests that the combustion reactions are controlled by the accessibility of the O₂ towards the vicinity of the residual solid, and during the two previous stages, the high release of H₂O, CO₂, CO, CH₄ and volatile organic compounds, apparently limits the O₂ accessibility and the reaction preferentially occur in gas phase. It explains why the reactions are not thermally auto-catalyzed during combustion process, although the reactions are strongly exothermic under experimental condition used in this study.

Acknowledgements We gratefully acknowledge that this work was supported by the Instituto Mexicano del Petroleo (IMP), project: D.00463 and DGAPA project IN115708-3. The authors would like to thank Paula Vera-Cruz Dutrenit for the style correction of the manuscript.

References

1. Subramani V, Gangwal SK. A review of recent literature to search for an efficient catalytic process for the conversion of syngas to ethanol. *Energy Fuels*. 2008;22(2):814–9.
2. Phillips SD. Technoeconomic analysis of a lignocellulosic biomass indirect gasification process to make ethanol via mixed alcohols synthesis. *Ind Eng Chem Res*. 2007;46(26):8887–97.
3. Swami SM, Abraham MA. Integrated catalytic process for conversion of biomass to hydrogen. *Energy Fuels*. 2007;20(6):2616–22.
4. Calvo LF, Sánchez ME, Morán A, García AI. TG-MS as a technique for a better monitoring of the pyrolysis, gasification and combustion of two kinds of sewage sludge. *J Therm Anal Calorim*. 2004;78(2):587–98.
5. Li SG, Xu SP, Liu SQ, Yang C, Lu QH. Fast pyrolysis of biomass in free-fall reactor for hydrogen-rich gas. *Fuel Process Technol*. 2004;85(8–10):1201–11.
6. Mohan D, Pittman CU Jr, Steele PH. Pyrolysis of wood/biomass for bio-oil: a critical review. *Energy Fuels*. 2006;20(3):848–89.

7. Yang H, Yan R, Chen H, Zheng C, Lee DH, Liang DT. In-depth investigation of biomass pyrolysis based on three major components: hemicellulose, cellulose and lignin. *Energy Fuels*. 2006;20(1):388–93.
8. Kleinert M, Barth T. Towards a lignin-cellulosic biorefinery: direct one-step conversion of lignin to hydrogen-enriched biofuel. *Energy Fuels*. 2008;22(2):1370–9.
9. van Rossum G, Kerten SRA, van Swaaij WPM. Catalytic and noncatalytic gasification of pyrolysis oil. *Ind Eng Chem Res*. 2007;46(12):3959–67.
10. Jiménez A, Ruseckaite R. Binary mixtures based on polycaprolactone and cellulose derivatives. *J Therm Anal Calorim*. 2007;88(3):851–6.
11. Khelifa A, Fiqueneisel G, Auber M, Weber JV. Influence of some minerals on the cellulose thermal degradation mechanisms. *J Therm Anal Calorim*. 2008;92(3):795–9.
12. Torres-García E, Balmaseda J, del Castillo LF, Reguera E. Thermal evolution of microporous nitroprussides on their dehydration process. *J Therm Anal Calorim*. 2006;86(2):371–7.
13. Yang H, Yan R, Chen H, Lee HD, Zheng C. Characteristics of hemicellulose, cellulose and lignin pyrolysis. *Fuel*. 2007;86(12–13):1781–8.
14. Mckendry P. Energy production from biomass (part 1): overview of biomass. *Bioresour Technol*. 2002;83(1):37–46.
15. Demirbas A. Mechanisms of liquefaction and pyrolysis reactions of biomass. *Energy Convers Manag*. 2000;41(6):633–46.
16. Shanmukharadhya KS. Simulation and thermal analysis of the effect of fuel size on combustion in an industrial biomass furnace. *Energy Fuels*. 2007;21(4):1895–900.
17. Soltes EJ, Elder TJ. Pyrolysis. In: Goldstain IS, editor. *In organic chemicals from biomass*, Chapter 5. Boca Raton: CRC Press; 1981. p. 63–99.
18. Pouchert ChJ, editor. *The Aldrich Library of FT-IR spectra vapor phase*. Milwaukee: Aldrich Chemical Company; 1989, vol. 3, Chapter. Non-Aromatic Alcohols, p. 155–263 and Chapter. Non-aromatic anhydrides, p. 759–63.
19. Nair SA, Nozaki T, Okazaki K. In situ Fourier transform infrared (FTIR) study of nonthermal-plasma-assisted methane oxidative conversion. *Ind Eng Chem Res*. 2007;46(11):3486–96.
20. Vyazovkin S, Wight CA. Kinetics in solids. *Annu Rev Phys Chem*. 1997;48:125–49.
21. Vyazovkin S, Wight CA. Model-free and model-fitting approaches to kinetic analysis of isothermal and nonisothermal data. *Thermochim Acta*. 1999;341:53–68.
22. Rodríguez-Gattorno G, del Castillo LF, Torres-García E. Combined used of high resolution TGA with the isoconversion method: kinetic analysis of the thermal dehydration of $\text{KNbWO}_6 \cdot \text{H}_2\text{O}$. *Thermochim Acta*. 2005;435:176–80.
23. Aleman-Vazquez LO, Torres-García E, Rodríguez-Gattorno G, Ocotlan-Flores J, Camacho-Lopez MA, Cano JL. Oxidation process of MoO_xC_y to MoO_3 : kinetics and mechanism. *J Solid State Chem*. 2004;177:3281–9.